

## Characterization and Isolation of Intermediates in $\beta$ -Lactoglobulin Heat Aggregation at High pH

Rogert Bauer,\* Rita Carrotta, Christian Rischel, and Lars Øgendal

Department of Physics, Royal Veterinary and Agricultural University, DK-1871 Frederiksberg C, Denmark

**ABSTRACT** The early stages of heat induced aggregation at 67.5°C of  $\beta$ -lactoglobulin were studied by combined static light scattering and size exclusion chromatography. At all conditions studied (pH 8.7 without salt and pH 6.7 with or without 60 mM NaCl) we observe metastable heat-modified dimers, trimers, and tetramers. These oligomers reach a maximum in concentration at about the time when large aggregates (1000–4000 kg/mol) appear, after which they decline in concentration. By isolating the oligomers it was demonstrated that they rapidly form aggregates upon heating in the absence of monomeric protein, showing that these species are central to the aggregation process. To our knowledge this is the first time that intermediates in protein aggregation have been isolated. At all stages of aggregation the dominant oligomer was the heat-modified dimer. Whereas the heat-modified oligomers are formed at a higher rate at pH 8.7 than at pH 6.7, the opposite is the case for the formation of aggregates from the metastable oligomers indicating cross-linking via disulfide bridges for the oligomers and noncovalent interaction in the formation of the aggregates. The data suggest that an aggregate nucleus is formed from four oligomers. For protein concentrations of 10 or 20 g/l a heat-modified monomer can be observed until about the time when the maximum in concentration appears of the heat-modified dimer. The disappearance of this heat-modified monomer correlates to the formation of dimers (trimers and tetramers).

### INTRODUCTION

The study of protein aggregation has for many years been important in relation to food production and biotechnology. In recent years, the implication of protein aggregates in a number of diseases has brought renewed interest to the field. In some cases aggregation proceeds by random sticking together of the molecules, leading to unstructured aggregates; in other cases the proteins form specific contacts, leading to aggregates of well-defined structures. Studies have shown that many quite different proteins form a highly structured type of aggregates known as amyloid, characterized by a high content of  $\beta$ -sheet and with the shape of rods (fibrils) or plaques (Dobson, 1999). The structural events that initiate aggregation therefore may be expected to show common traits. The characterization of these structural changes, however, has proven to be quite difficult. The most detailed mechanism that has been discussed is probably the strand insertion deduced for  $\alpha$ -antitrypsin by Elliot et al. (1996), who also conjectured a model for the amyloid fibril. Fiber diffraction data have been obtained from transthyretin amyloid fibrils (Blake and Serpell, 1996), suggesting for this system a rather different structure consisting of four very long  $\beta$ -sheets. Model systems in which the aggregation process can be arrested at early times in a controlled fashion might give new possibilities to study the characteristics of structured aggregation.

$\beta$ -lactoglobulin is the major protein component in bovine whey, and belongs to the retinol binding family of proteins showing a  $\beta$ -sandwich and one long  $\alpha$ -helix (Brownlow et al., 1997). Upon heating to temperatures above 60°C the  $\alpha$ -helix unfolds while the  $\beta$ -sheet remains intact, and the protein molecules subsequently aggregate. When the sample is cooled in ice water the aggregation stops, and in this way the process can be easily monitored. Aggregates formed at low ionic strength appear to be open, thin-stranded structures (Foegeding et al., 1995) and the large content of  $\beta$ -sheet structure in  $\beta$ -lactoglobulin suggests that there may be structural similarities with the processes implicated in formation of amyloid, although this is not known with certainty. Several studies (Aymard et al., 1999; Elofsson et al., 1996; Haque and Sharma, 1997; Hoffmann et al., 1996) have been performed in order to elucidate the structure of the aggregates appearing after heating of  $\beta$ -lactoglobulin. The primary cause of initiation of heat aggregation is thought to involve disulfide bridge formation by exchange between the free thiol group and one of the two disulfide bridges (Shimada and Cheftel, 1989; Sawyer, 1967). Roefs and de Kruif (1994) have proposed a model in which disulfide formation occurs throughout the aggregation process. However, whether this is in fact the case has never been proven. Indication of the importance of a disulfide-linked dimer was given in Manderson et al. (1999). In the present work, we use combined size exclusion chromatography and light scattering to study heat-induced aggregation of  $\beta$ -lactoglobulin at high pH and low salt concentration. The results show that the aggregation proceeds through the formation of metastable heat-modified dimers and higher oligomers, which form the basis for further aggregation. The isolation of the metastable intermediates

Received for publication 7 February 2000 and in final form 8 May 2000.

Address reprint requests to Dr. Rogert Bauer, Royal Veterinary & Agricultural University, Dept. of Physics, Thorvaldsensvej 40, DK-1871 Frederiksberg C, Denmark. Tel. 45-35-28-23-07; Fax: 45-35-28-23-50; E-mail: rba@kv1.dk.

© 2000 by the Biophysical Society

0006-3495/00/08/1030/09 \$2.00

done in this work provides a powerful approach to the elucidation of the structural basis of aggregation.

## MATERIALS AND METHODS

### Sample preparations

All chemicals used were of analytical grade. All water used was purified using an Elga Maxima system. All samples were prepared, dialyzed against and heat-treated in a 10 mM  $\text{Na}_2\text{HPO}_4$  buffer, pH 8.7 or pH 6.7 with or without 60 mM NaCl.  $\beta$ -Lactoglobulin A and B were obtained from Sigma as dried powder. To prepare the samples for the measurements, different amounts of dry powder of each sample was dissolved in 2.5 ml of buffer and subsequently dialyzed against 1 l of buffer at 4°C under stirring for 8 h and then, after a change of buffer, for another 16 h. After dialysis the samples were diluted to the appropriate concentration in the buffer and filtered twice through the same 200 nm pore filter into two dust-free test tubes, 1 ml in each. The protein concentration was determined by UV absorbance using an extinction coefficient of  $0.96 \text{ l g}^{-1} \text{ cm}^{-1}$ . For simultaneous light scattering and size exclusion chromatography 75  $\mu\text{l}$  was extracted at regular intervals from the sample in the water bath and taken in an Eppendorf tube to an ice bath for thermal quenching.

### Simultaneous static light scattering, refractive index measurements, and size exclusion chromatography

Samples were injected containing 0.5 mg of protein, except for the dilution series, was injected into a SUPERDEX 200  $7.8 \times 300 \text{ mm}$  column having a flow of 0.5 ml/min. The sample injected was either 50  $\mu\text{l}$ , 10 g/l  $\beta$ -lactoglobulin or 500  $\mu\text{l}$ , 1 g/l  $\beta$ -lactoglobulin. For the dilution series 500  $\mu\text{l}$  injection was used and the concentration given refers to this. The column was equilibrated in 10 mM  $\text{NaH}_2\text{PO}_4/\text{Na}_2\text{HPO}_4$  pH 6.7, 60 mM NaCl. After having passed through the column the sample ran first through the light scattering instrument (Dawn F with a K2 cell, Wyatt Technology, Santa Barbara, CA), and then through the refractive index detector (RID-10A, Shimadzu, Japan or Wyatt Optilab 903, Wyatt Technology, Santa Barbara, CA). All flow measurements were done at a temperature of 20°C, controlled via a water bath. The concentration of the species appearing in the elution profiles was determined by measurement of the refractive index. Bovine serum albumin from Sigma was applied to the column in order to calibrate the light scattering detectors. In order to estimate the molar mass, and radius of gyration for the aggregates, a Debye plot, i.e., light scattering signal vs.  $q^2$  was made (the light intensities were measured at 15 angles out of which 10 were used in a  $q$  range of  $10\text{--}25 \mu\text{m}^{-1}$ ). The radius of gyration was derived from the slope of this line and the weight average molecular mass was obtained by the intercept at the ordinate axis divided by the refractive index signal. For the oligomers with mass less than 100 kg/mol the light scattering was isotropic and only one angle was used for mass determination. When samples needed to be concentrated it was accomplished by centrifugation through an Amicon filter with a 5 kg/mol cutoff.

## RESULTS

### Size distributions during heat aggregation

The time course of aggregation during heating was followed under different conditions as given in Table 1. In Fig. 1 is shown the refractive index signal as a function of the elution volume at several different heating times. The samples were 10 g/l of  $\beta$ -lactoglobulin A and B, dissolved in 10 mM phosphate buffer, pH 8.7 heated at 67.5°C. From this figure

**TABLE 1** Experimental conditions for heating at 67.5°C in 10 mM phosphate buffer

Concentration $\beta$ -lactoglobulin (g/l)	pH	NaCl (mM)	Variant
10	8.7	0	A
20	8.7	0	A
50	8.7	0	A
105	8.7	0	A
10	8.7	0	B
14	6.7	60	A
10	6.7	0	A

it is seen that for both variants a variety of oligomers including the monomer appear (from about 14 to 18 ml elution volume) at all shown heating times. The molar mass of the oligomers have been determined from light scattering as described in materials and methods sections. This is illustrated in Fig. 2. The identification of the various oligomers is indicated by arrows in Fig. 1. Peaks with molar masses of the monomer, dimer, and trimers are observed for both variants. A tetramer is present at low concentration for both variants and can be identified as a peak for the B variant to the left of the trimer position. The positions of the dimer, trimer and tetramer are independent of the heating time. In contrast, molecules appearing between the dimer and monomer position vary in position and mass between the monomer and dimer. In accordance with this, the mass and peak position of the unheated protein are slightly lower than that of the dimer (Fig. 2). At heating times from 15 to 180 min at volumes between 16 to 18 ml (Fig. 1), intensity composed of two partly overlapping peaks appears of which the left part represents the monomer. At later heating times, a single broad band appears with a slow decrease in mass toward the mass of the monomer with increasing heating times. The disappearance of the monomer peak observed up to 180 min correlates to the presence of the dimers, trimers, and tetramers. This behavior is observed for both variants (Fig. 1).

The behavior of the two variants when heated is almost identical concerning the types of oligomers. From 375 min and later aggregates appear for both variants. Correlated to this is a gradual decrease in the concentration of dimers, trimers, and tetramers. For the A variant the oligomers change suddenly into the aggregates in contrast to the B variant where the oligomers gradually turn into the aggregates between 60 and 1527 min (Fig. 1).

In Fig. 3 are shown elution profiles for the refractive index signal for different pH values, NaCl, and protein concentrations. The heating times for the different profiles were selected such that the concentration of large aggregates was roughly the same for all shown cases. It can be seen that the metastable oligomers appear under all conditions shown, although in different concentration.

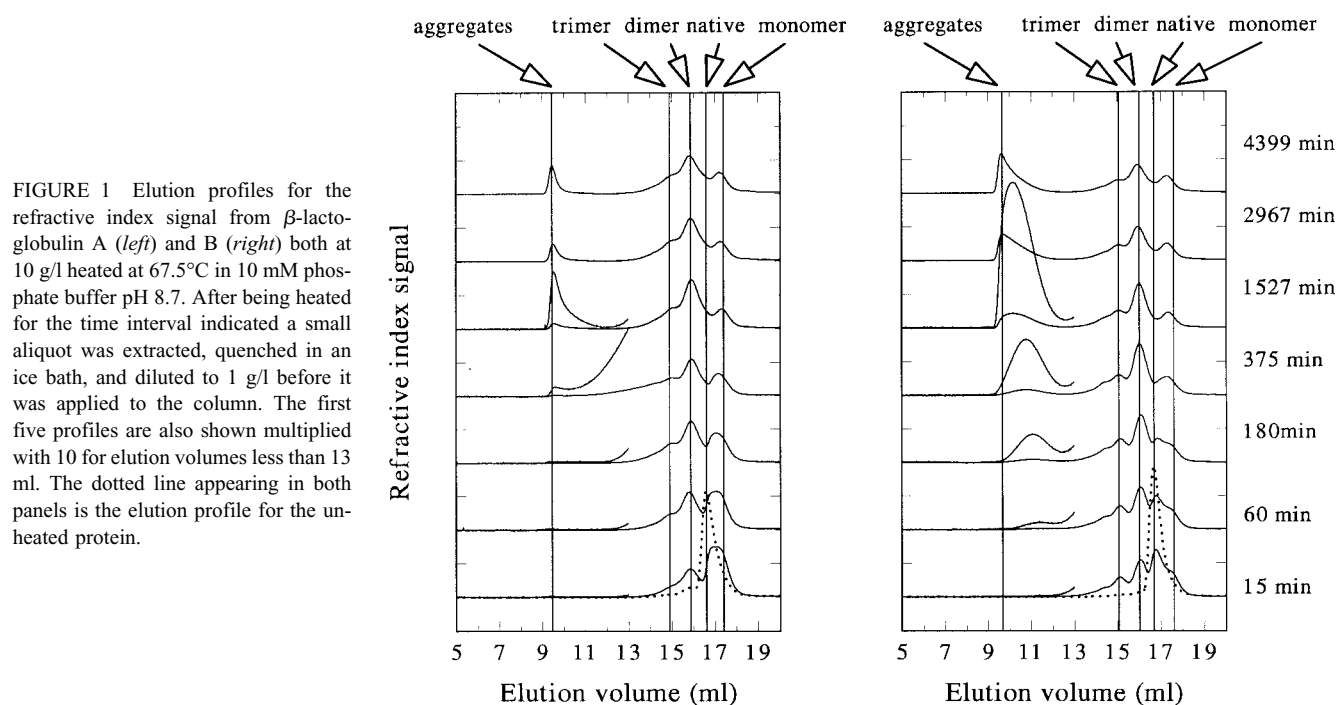


FIGURE 1 Elution profiles for the refractive index signal from  $\beta$ -lactoglobulin A (left) and B (right) both at 10 g/l heated at 67.5°C in 10 mM phosphate buffer pH 8.7. After being heated for the time interval indicated a small aliquot was extracted, quenched in an ice bath, and diluted to 1 g/l before it was applied to the column. The first five profiles are also shown multiplied with 10 for elution volumes less than 13 ml. The dotted line appearing in both panels is the elution profile for the unheated protein.

In Fig. 4 plots are shown of the radii of gyration for the aggregates for the A and B variants heated at pH 8.7 with samples containing 10 g/l  $\beta$ -lactoglobulin (Table 1) in the time range of 1500 to 5000 min. For the A variant an average radius of gyration of  $29 \pm 1$  nm and molar mass

increasing from 2000 to 3500 are derived and for the B variant an average radius of gyration of  $21 \pm 2$  nm and molar mass increasing from 800 to 1300 kg/mol are derived.

### Isolated oligomers

The question arises whether or not the aggregates present between 9 and 10 ml and the oligomers present between 13 and 18 ml elution volumes can dissociate or associate depending on their concentration. To study this, we made size exclusion with a 20 g/l  $\beta$ -lactoglobulin A solution at pH 8.7

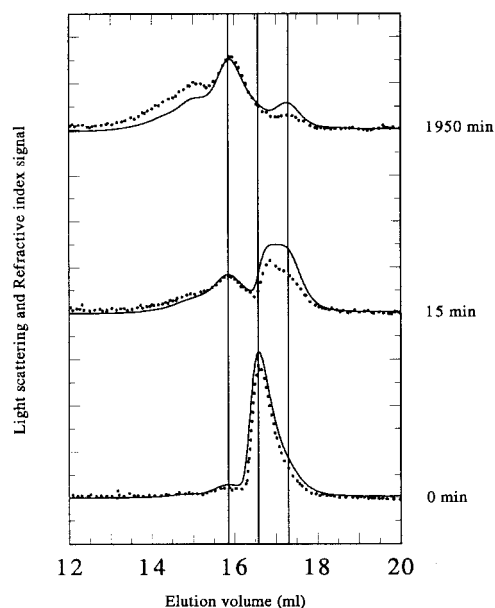


FIGURE 2 Oligomer region close up: Light scattering (at  $q = 20.7 \mu\text{m}^{-1}$ , dotted lines) and refractive index signal (solid lines) for 10 g/l for the A variant after 0, 15 and; 1950 min of heating. The light scattering signal is scaled to the same value as the refractive index signal at the peak for the metastable dimer.

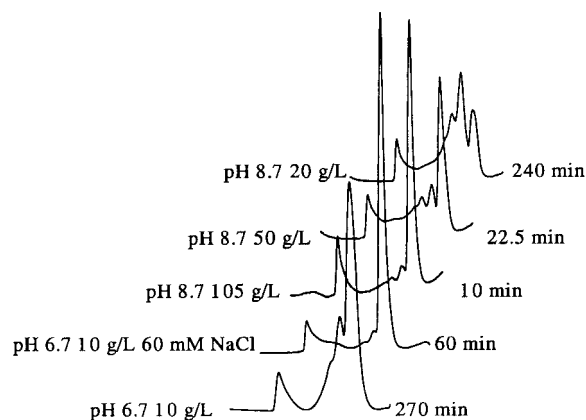


FIGURE 3 Refractive index signals for different conditions chosen at heating times for the first appearance of the aggregate peaks but such that the concentration is roughly the same. The leftmost peaks are from the aggregates, the rightmost peaks from the monomer/dimer.

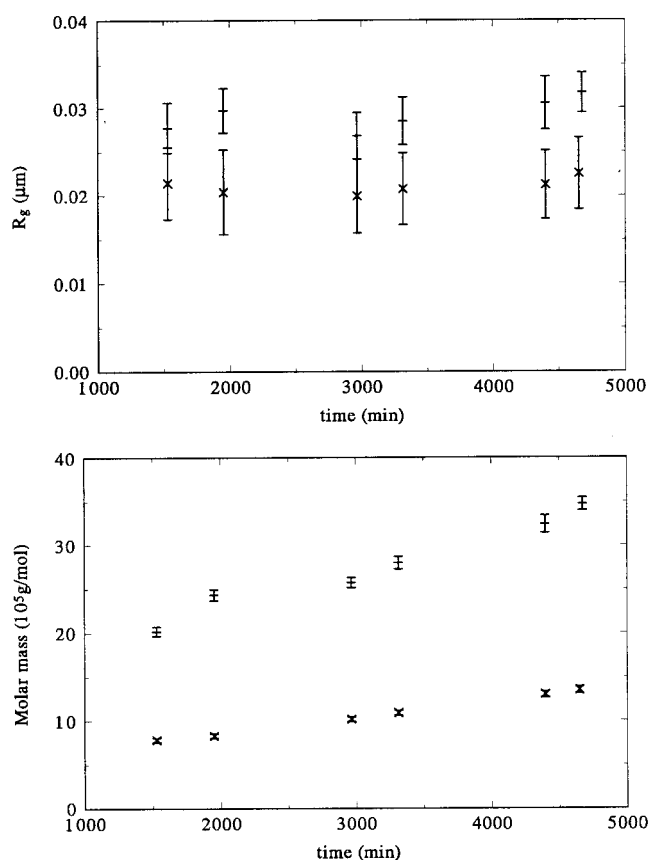


FIGURE 4 Molar mass and radius of gyration of aggregates from 10 g/l  $\beta$ -lactoglobulin A and B heated at 67.5°C in 10 mM phosphate buffer pH 8.7 for various lengths of time. The data are evaluated in the  $q$  range 8 to 25  $\mu\text{m}^{-1}$  by fitting a straight line to the light scattering signal normalized by the refractive index signal in a Debye plot. The dash represents the A variant and the cross-the B variant.

after 105 min heating, applying different concentrations of the sample to the column. The corresponding elution profiles are shown in Fig. 5. From this figure it is evident that no dissociation occurs upon dilution for the aggregates. Furthermore, in the region of the dimer and trimer peaks including higher oligomers, it can be seen that at the highest concentrations, i.e., 10 and 20 g/l, some association occurs shifting the distributions of oligomers toward higher multimers. However the peak positions of the dimer and trimer are stable toward dilution and these oligomers show no dissociation toward the monomer. These oligomers we therefore denote as metastable because they do not dissociate. This is in contrast to the molecules appearing in the peak at the monomer position at 0.1 g/l but shifted toward lower volumes upon increasing the concentration. From analysis of the light scattering intensity (Table 2) the molar mass in this peak is raising with protein concentration from being close to the monomer toward being close to the dimer. This clearly shows a reversible dissociation/association equilibrium between the monomer and the dimer for this

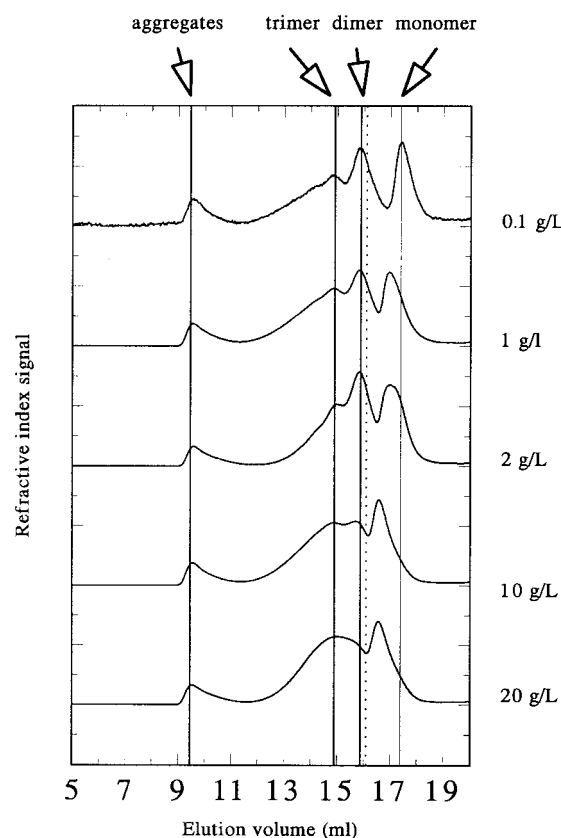


FIGURE 5 Elution profiles for the refractive index signal from 20 g/l  $\beta$ -lactoglobulin A heated at 67.5°C in 10 mM phosphate buffer pH 8.7 for 105 min and subsequently quenched in an ice bath. 500  $\mu\text{l}$  of the heated sample having the protein concentration given in the figure was applied to the column. For the diluted samples a 10 mM phosphate buffer pH 8.7 was used for dilution. The elution profiles were normalized to give the same area independent of dilution.

peak. The molecule present in this mobile peak we therefore denote the labile monomer/dimers. The consequence of the results discussed above is that two forms of a  $\beta$ -lactoglobulin dimer exist, one which is stable toward dissociation to the monomer and one which does dissociate to the monomer upon dilution. In order to further establish the behavior

TABLE 2 Molar mass vs. concentration derived from the dilution series shown in Figure 7

Concentration (g/l)	Native molar mass (kg/mol)	Heated molar mass (kg/mol)	Native elution volume (ml)	Heated elution volume (ml)
0.1	22	25	17.1	17.2
0.2	21	29	17.0	17.0
0.5	25	31	16.8	16.8
1.0	29	34	16.7	16.7
2	30	32	16.5	16.5
5	31	32	16.5	16.4

Molar mass shown is weight average molar mass.

observed in Fig. 5 and to characterize the aggregation properties of the metastable oligomers and the monomer/dimer molecules we fractionated the oligomers appearing from the elution profile for 20 g/l (bottom profile in Fig. 5). The oligomers were separated into two groups: a fraction here denoted the metastable oligomers was collected from 13 to 16.1 ml and a fraction denoted the monomer/dimer fraction from 16.1 to 18 ml. The choice of 16.1 ml as the separating volume for the two collected fractions was made from the minimum observed in the profiles for 20 g/l (Fig. 5, *dotted line*). In order to have enough material for the dilution series with the isolated oligomers, 500  $\mu$ L of the 20 g/l solution was applied to the column four times. The two collected fractions were then concentrated to 10 g/l and dilution series, with regard to the protein concentration injected in the column, were made on each fraction, together with a dilution series for the unheated protein. The results are shown in Figs. 6 and 7. Again it is seen (Fig. 6) that the aggregates and oligomers (molecules appearing up to 16.6 ml) are virtually unaffected by dilution except that the

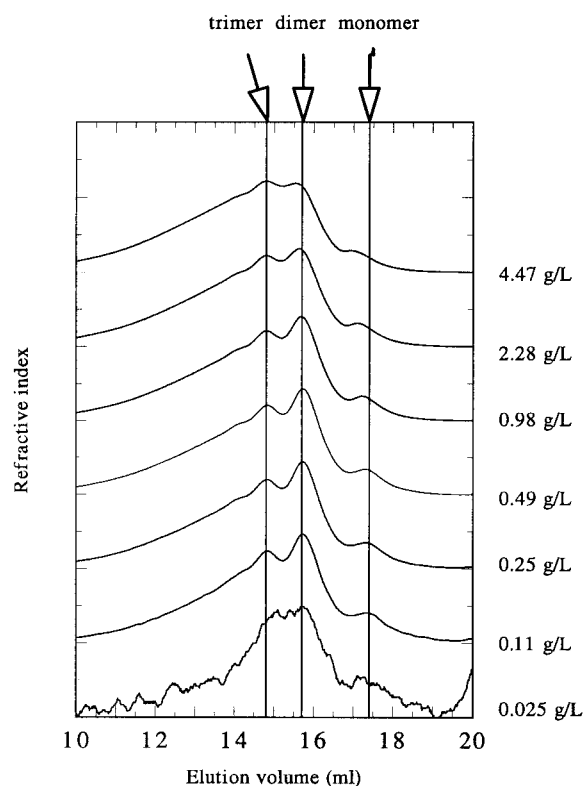


FIGURE 6 Elution profiles for the refractive index signal for a dilution series of the oligomer fraction. The oligomer fraction sample was generated by heating 20 g/l  $\beta$ -lactoglobulin A at 67.5°C for 105 min in 10 mM phosphate buffer pH 8.7 for 105 min. After heating the sample was quenched in an ice bath and then four times 500  $\mu$ L was applied to the column (see lower curve in Fig. 5) and the material from 13 to 16.1 ml was collected. The resulting material was concentrated to 10 g/l. The elution profiles shown are normalized to give the same area independent of dilution.

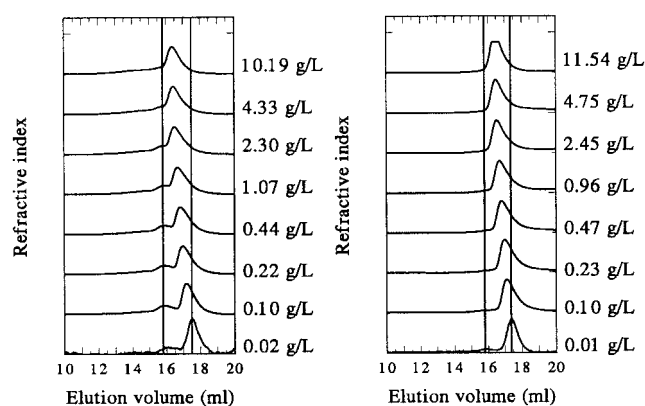


FIGURE 7 Elution profiles for the refractive index signal for a dilution series of the monomer/dimer fraction (*left*). The monomer/dimer fraction was chosen from the column elution described in the legend to Fig. 6 by collecting the material from 16.1 ml to 18 ml. For comparison elution profiles for a dilution series of unheated protein are also shown (*right*). The elution profiles were normalized to give the same area independent of dilution.

oligomers exhibit a trend to further association at the highest concentrations. Below 2 g/l or  $10^{-4}$  M, the shape of the elution profile is constant. Long time storage (order of days at 4°C) initiates a slow aggregation but no dissociation of the metastable oligomers (data not shown). In contrast to this, the molecules appearing between about 16 and 18 ml, having molar mass between the monomer and dimer (Fig. 7 and Table 2), appear at increasing volume with increasing dilution. This is the case for both the heated and unheated dilution series (Fig. 7 and Table 2). This means that these molecules exhibit a monomer/dimer equilibrium which is fast relative to the column passage time. From the weight average molar mass shown in Table 2 the dissociation constant is estimated to be about  $1 \times 10^{-5}$  M and  $5 \times 10^{-5}$  M for the heated and unheated sample respectively. These estimates are based on the fact that when the molar concentration of monomers and dimers is equal, the molar mass is 5/3 (weight average) times the monomer mass. The total applied concentration for which this occurs is 2 g/l and 0.5 g/l for the native and heated protein respectively. As the average dilution factor during column passage is 2, the concentrations used for calculating the equilibrium constants are chosen as half of these values. Note that the equilibrium constants relates to pH 6.7 10 mM phosphate buffer containing 60 mM NaCl, i.e., the column buffer. The conclusion is that the monomer/dimer fractions for both the heated and unheated samples exhibit a monomer/dimer equilibrium with perhaps slightly different equilibrium constants.

### Kinetics of aggregation

To visualize the kinetic behavior of the different molecular entities, we integrated three areas in the refractive index



elution profiles shown in Fig. 1. Fig. 8 shows the results. It can be seen that before the formation of aggregates, a lag phase of about 200 min exists for the A variant. At the end of this lag phase the metastable oligomers have reached a maximum in concentration. However, the B variant shows no lag phase for aggregate formation. In particular, the B variant shows a correlation between the formation of the aggregates and a decline in the concentration of the metastable oligomers. Although the low concentration of the aggregates within the time window shown in Fig. 8 obscures the picture for the A variant, the same correlation is found at later times (data not shown).

The influence of total protein concentration on the appearance of metastable oligomers and aggregates is shown in Fig. 9 (see legends for details). For the aggregates we made a linear fit to the concentration of aggregates as a function of heating time in the time window shown in Fig. 9, lower panel, to derive initial rates of aggregation after the lag phase. This initial rate is plotted as a function of concentration of total  $\beta$ -lactoglobulin in Fig. 10. A fit to the

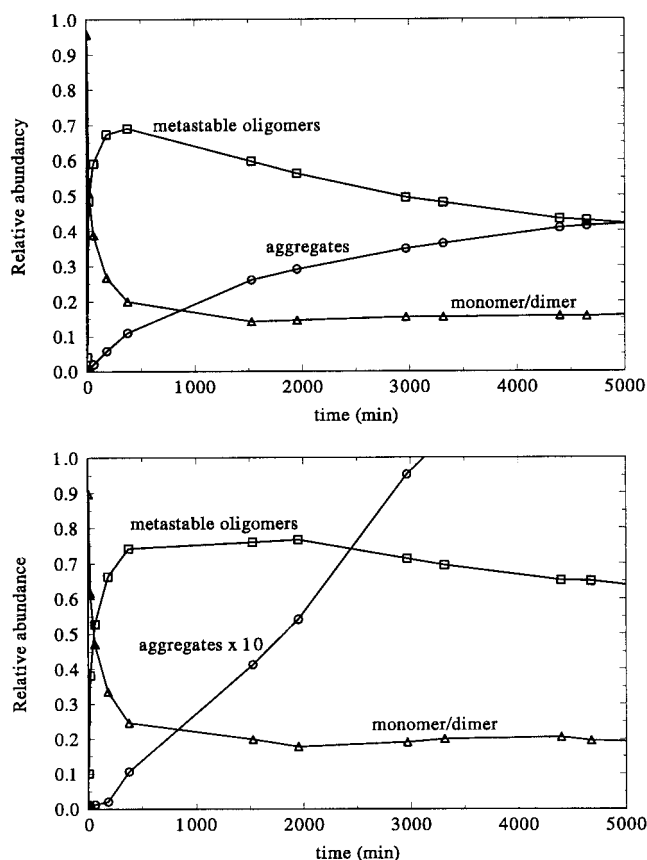


FIGURE 8 The refractive index signals shown in Fig. 1 were integrated in three areas for each time of heating. The sum of the three areas is normalized to 1. Shown are: aggregates (9.0 to 13 ml, circles), the metastable oligomers (13 to 16.6 ml, squares), and the labile monomer/dimer (16.6 to 18 ml, triangles). Lower panel, the A variant and upper panel, the B variant.

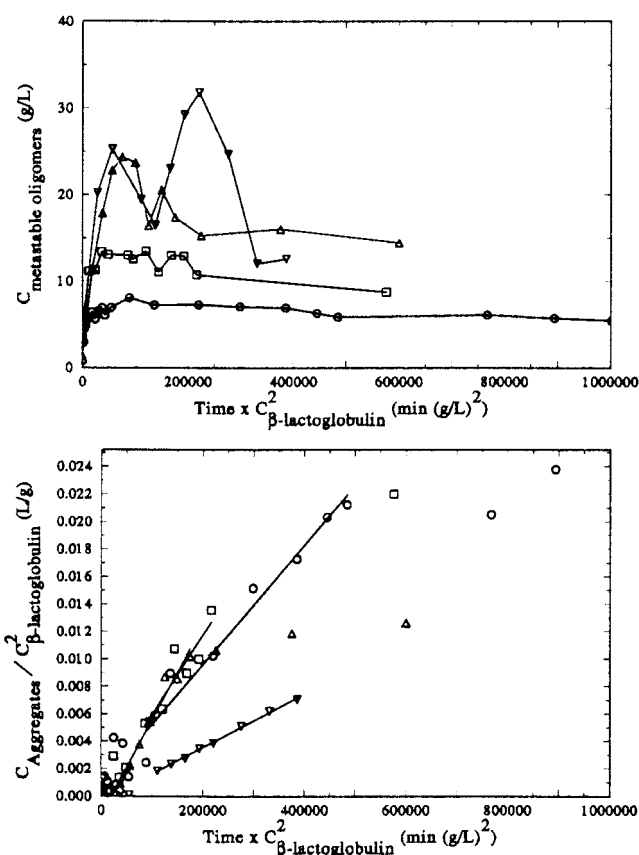


FIGURE 9 Concentration of aggregates (lower panel) and metastable oligomers (upper panel) as a function of heating time derived from the integration of the refractive index signals, as described in the legend to Fig. 8, from  $\beta$ -lactoglobulin A heated at 67.5°C in 10 mM phosphate buffer pH 8.7 at 105 g/l, 50 g/l, 20 g/l and 10 g/l. The time scales for the curves are rather different, so in order to present the curves simultaneously, the time was multiplied by the square of the total protein concentration (horizontal axis) and the concentration of the aggregates was divided by the square of the total protein concentration (vertical axis, lower panel). The symbols represent: circles, 10 g/l; squares, 20 g/l; up triangles, 50 g/l; down triangles, 105 g/l. The lines in the upper panels are guidelines to the eye and in the lower panel linear fits to the data shown in the range they are fitted to.

first three points with a power law gave an exponent of  $4.3 \pm 0.1$ . It can be seen that at 105 g/l the rate ( $\text{min}^{-1} \text{g}^{-1}$ ) is significantly slowed down. By averaging the concentration of the metastable oligomers (excluding the unheated case) values of about  $6 \pm 1$ ,  $12 \pm 2$ ,  $18 \pm 4$  and  $21 \pm 7$  g/l are reached for heating with 10, 20, 50, and 105 g/l, respectively (Fig. 9).

The two fractions collected (see above) were also tested for their ability to aggregate. This was done by heating again at 67.5°C in 10 mM phosphate buffer pH 6.7 and 60 mM NaCl. The kinetics of aggregation for the labile monomer/dimer fraction shown in Fig. 11 resembles that of heating native  $\beta$ -lactoglobulin under the same conditions. In contrast to this, the metastable oligomer fraction turned into

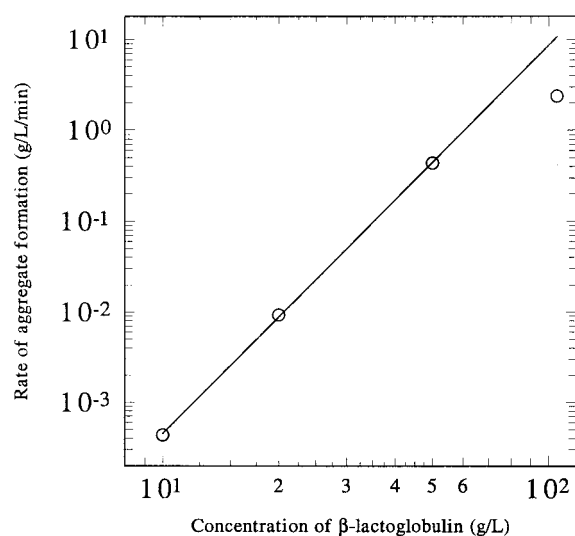


FIGURE 10 The lines shown in Fig. 9, lower panel, are converted to reaction rates and a linear fit was made (solid line). Only the first three points were used in the fit in a double logarithmic plot of rate vs. concentration.

aggregates at a much faster rate (Fig. 11). The absence of a lag phase for the monomer/dimer fraction is explained by a 20% presence of the metastable oligomers due to the imperfect separation of the two groups of molecules.

A comparison between a 10 g/l  $\beta$ -lactoglobulin A solution heated at either pH 6.7 or 8.7 shown in Fig. 12 demonstrates that the metastable oligomers are formed at a higher rate and to a higher concentration at pH 8.7 than at pH 6.7. In contrast, the rate is much faster for the formation of aggregates at pH 6.7 than at pH 8.7.

## DISCUSSION

### Intermediate oligomers

A study of heat denaturation of  $\beta$ -lactoglobulin with combined static light scattering and size exclusion chromatography, as we have done in this work, was recently performed by Hoffmann et al. (1997), but only covering the very late stages after heating thus preventing a study of the initial lag phase behavior of the aggregation. By studying the early stages of heating, Bauer et al. (1998) showed that small oligomers were reaction intermediates with respect to heat aggregation of  $\beta$ -lactoglobulin. From the work presented here it follows that the intermediate molecules appearing at pH 8.7 with no salt also appear at pH 6.7, with or without 60 mM NaCl, the difference being the concentration and time course of formation of the different oligomers (Figs. 3 and 12). This shows that relevant details of the early stages of heat aggregation can be revealed and their entities be isolated by studying the aggregation at pH 8.7 where the

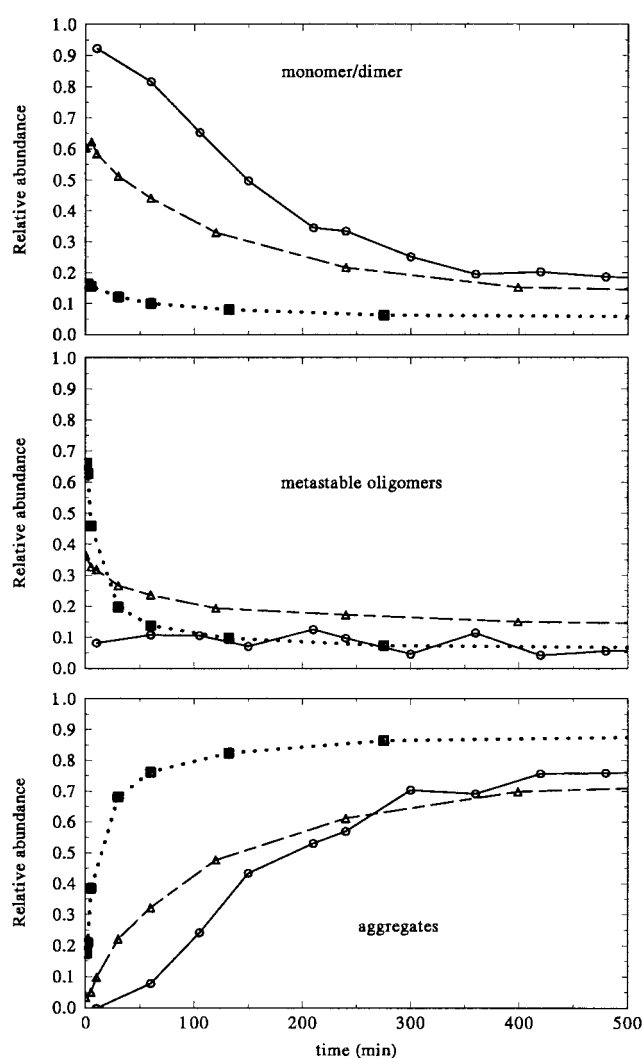


FIGURE 11 Time dependencies of the refractive index signals from three samples all heated at 67.5°C for different lengths of time in 10 mM phosphate buffer pH 6.7 containing 60 mM NaCl. The samples heated and quenched were: 14 g/l  $\beta$ -lactoglobulin A (circles, see Table 1); metastable oligomer fraction (squares) and monomer/dimer fraction (triangles) both at a concentration of 10 g/l  $\beta$ -lactoglobulin A (see figure legends to Fig. 6 and 7). The signals are integrated in three different areas. The sum of the three areas is normalized to 1.

build up of intermediate oligomers is conveniently slow at or below concentration of 20 g/l.

From the time course of heat aggregation at 10 g/l for the A and B variant several interesting features are revealed. Even at the first time observed after heating, a band composed of metastable oligomers is present. Although the heat-modified dimer is the most abundant oligomer, there are also trimers and tetramers present. The fact that the distribution between different metastable oligomers (dimers, trimers, and tetramers) is independent of the concentration applied to the column below 2 g/l, gives evidence for the formation of interprotein disulfide bridges since they

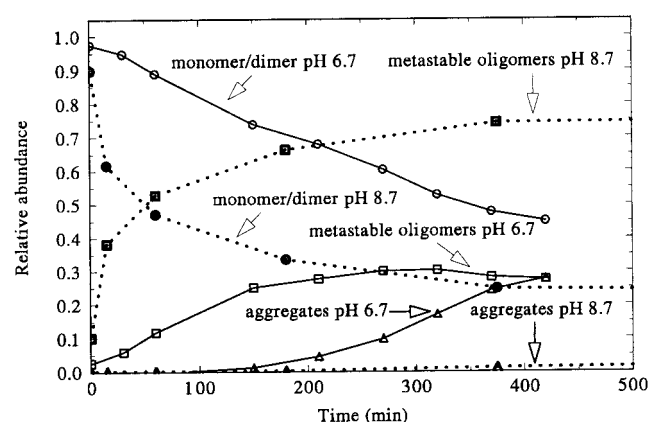


FIGURE 12 Time dependencies of the refractive index signals integrated in three different areas. The data shown are from the samples collected from 10 g/l  $\beta$ -lactoglobulin A heated at 67.5°C in 10 mM phosphate buffer pH 6.7 (solid lines) and pH 8.7 (dotted lines) for different lengths of time. The signals are integrated in three different areas. The sum of the three areas is normalized to 1.

are not supposed to dissociate by dilution. The existence of disulfide bridged oligomers was shown by electrophoresis studies by Manderson et al. (1999).

A plateau and a shoulder at 17.3 ml with a mass of the monomer can be observed up to 180 min of heating (Fig. 1). This could be a reactive monomer with the cysteine exposed for disulfide formation (Manderson et al., 1999). Much work has focused on the role of the free thiol group (cys121) in  $\beta$ -lactoglobulin (see for example Sawyer, 1967; Shimada and Cheftel, 1989; Xiong et al., 1993; Hoffman and van Mil, 1997). The aggregation kinetics and the aggregate structure also differ with the presence or absence of the thiol blocking group *N*-ethylmaleimide (Hoffmann and van Mil, 1997). The proposed mechanism of the free thiol group is that after heat activation it is capable of building oligomers by disulfide bond switch with one of the two disulfide bridges in  $\beta$ -lactoglobulin. A mechanism based on this has been proposed (Roefs and de Kruif, 1994). Griffin and Griffin (1993) have proposed that at elevated temperatures the monomer becomes dominant such that in the model presented by Roefs and de Kruif (1994), the starting point is monomer-monomer interaction. This is in agreement with the observations made here.

From Fig. 1 it is seen that with an initial concentration of 10 g/l, most of the sample material has been converted to metastable oligomers before aggregation begins. This is also the case at 20 g/l (Fig. 3). Under these conditions, the rate of aggregation directly reflects the process of building aggregates from oligomers. An explanation of the slope of 4.3 of the linear fit to the first three points in Fig. 10 could be that below 50 g/l the reaction mechanism of aggregate formation from the metastable oligomers exhibits a cooperativity of 4.3, suggesting that the rate limiting step in aggregation is the formation of a nucleus of 4 metastable oligomers.

When the initial concentration is increased to 50 or 105 g/l, we move into conditions where a steady-state between production of oligomers from monomers and conversion into aggregates is rapidly reached. In this case, the rate of aggregation is limited by the production of oligomers, which proceeds by a reaction of order 2 or lower. This transition can be seen by the drop below the straight line for the rate for 105 g/l in Fig. 10, although the present data do not permit a quantitative analysis. The similar steady-state concentrations of oligomers ( $18 \pm 4$  g/l and  $21 \pm 7$  g/l) at total concentrations of 50 and 105 g/l reflects the high order of the aggregation reaction: When the rate of oligomer production is increased, only a small increase in the steady-state concentration is necessary to obtain a corresponding rate of aggregation. Taken together these data indicate the existence of a critical oligomer concentration of about 20 g/l needed for changing the rate limiting step from aggregation of oligomers to production of oligomers from monomers.

The hypothesis that aggregates are built from oligomers explain all our kinetic data. It is further supported by the fact that metastable oligomers in isolated form, rapidly aggregate without a lag phase upon heating (Fig. 11). All observations indicate that the aggregation mechanism is: monomer/dimer equilibrium  $\rightarrow$  activated monomer  $\rightarrow$  metastable disulfide linked dimers, trimers, and tetramers  $\rightarrow$  large aggregates.

This deviates from the model proposed by Roefs and de Kruif (1994) in which aggregates grow by addition of monomers through intermolecular disulfide bonds.

## Aggregates

At a concentration of 10 g/l aggregates with radius of gyration of 30 and 20 nm appear for the A and B variants, respectively (Fig. 4). In the time regime where the radius is constant the mass varies a factor of 1.8 and 1.6 for the A and B variant, respectively (Fig. 4), indicating compaction with increasing time. From Fig. 12 difference in behavior at pH 6.7 and 8.7 without NaCl is observed for the formation of the metastable oligomers and the formation of aggregates from the metastable oligomers. This indicates that these two processes proceed by different mechanisms in contrast to the model of Roefs and de Kruif (1994). The increase in the rate of formation of the metastable oligomer from pH 6.7 to 8.7 is consistent with cross-linking via disulfide bridges as discussed above, since disulfide bridge formation in general increases with pH. This is, however, not the case for the formation of the aggregates. As suggested by Manderson et al. (1999) other mechanisms such as hydrogen bonding and hydrophobic interactions are likely responsible for aggregate formation. The absence of metastable oligomers larger than the tetramer for the A variant supports this assertion.



## CONCLUSIONS

We have established that an important prerequisite for heat aggregation of  $\beta$ -lactoglobulin is the formation of heat-modified small oligomers ranging from dimers to tetramers. We have also shown that formation of the aggregates is different for the A and B variant. Whereas the A variant forms aggregates only after a lag time, the B variant starts immediately to form aggregates which gradually increase in size with increasing heating time until the size of about 21 nm is reached. We have further shown that the kinetics of formation of metastable oligomers are different from the kinetics of aggregate formation which suggests that the metastable oligomers are cross-linked by disulfide bonds and that the aggregates formed from the metastable oligomers most likely only contain the cross-links already present in the oligomers.

Although it is demonstrated that the aggregates at the conditions tested in this work need the same metastable oligomers to be formed, work from other groups have demonstrated that, in particular, the amount of salt present affects the nature of the aggregates formed. Thus, aggregates formed at low ionic strength appear to be open, thin stranded structures (Foegeding et al., 1995) in contrast to structures formed at salt concentrations larger than 0.1 M appearing much denser. It is thus possible that the aggregates formed at pH 8.7 where no salt is present have fibrillar structures formed from  $\beta$ -sheet rich structures like amyloid but for high salt concentration this might be different.

This work was supported by the European Commission through a grant to the concerted action on Molecular Basis of the Aggregation, Denaturation, Gelation and Surface Activity of Whey Protein, CT96-1202. Support of this work by the Danish Natural Science Council and the Carlsberg foundation is gratefully acknowledged. The authors are indebted to Marianne Lund Jensen for excellent help with sample preparations.

## REFERENCES

- Aymard, P., T. Nicolai, D. Durand, and A. Clark. 1999. Static and dynamic scattering of  $\beta$ -lactoglobulin aggregates formed after heat-induced denaturation at pH 2. *Macromolecules*. 32:2542-2552.

- Bauer, R., Hansen, S., and L. Øgdenal. 1998. Detection of intermediate oligomers, important for the formation of heat aggregates of  $\beta$ -lactoglobulin. *Int. Dairy J.* 8:105-112.
- Blake, C., and L. Serpell. 1996. Synchrotron x-ray studies suggest that the core of the transthyretin amyloid fibril is a continuous  $\beta$ -sheet helix. *Structure*. 4:989-998.
- Brownlow, S., J. H. M. Cabral, R. Cooper, D. R. Flower, S. J. Yewdall, I. Polikarpov, A. C. T. North, and L. Sawyer. 1997. Bovine  $\beta$ -lactoglobulin at 1.8 Å resolution—still an enigmatic lipocalin. *Structure*. 5:481-495.
- Dobson, C. M. 1999. Protein misfolding, evolution and disease. *Trends Biochem. Sci.* 24:329-332.
- Elliot, P. R., D. A. Lomas, R. W. Carrell, and I. P. Abrahams. 1996. Inhibitory conformation of the reactive loop of  $\alpha_2$ -antitrypsin. *Nat. Struct. Biol.* 3:676-681.
- Elofsson, U. M., P. Dejmk, and M. A. Paulsson. 1996. Heat-induced aggregation of  $\beta$ -lactoglobulin studied by dynamic light scattering. *Int. Dairy J.* 6: 343-357.
- Foegeding, E. A., E. L. Bowland, and C. C. Hardin. 1995. Factors that determine the fracture properties and microstructures of globular protein gels. *Food Hydrocolloids*. 9:237-249.
- Griffin, W. G., and M. C. A. Griffin. 1993. Time-dependent polydispersity of growing colloidal aggregates: predictions from dynamic light scattering theory. *J. Chem. Soc. Faraday Trans.* 89:2879-2889.
- Haque, Z. H., and M. Sharma. 1997. Thermal gelation of  $\beta$ -lactoglobulin AB purified from cheddar whey. 1. Effect of pH association as observed by dynamic light scattering. *J. Agric. Food Chem.* 45:2958-2963.
- Hoffmann, M. A. M., S. P. F. M. Roefs, M. Verheul, P. J. J. M. van Mil, and K. G. de Kruif. 1996. Aggregation of  $\beta$ -lactoglobulin studied by in situ light scattering. *J. Dairy Res.* 63:423-440.
- Hoffmann, M. A. M., G. Sala, C. Olieman, K. G. de Kruif. 1997. Molecular mass distributions of heat-induced  $\beta$ -lactoglobulin aggregates. *J. Agric. Food Chem.* 45:2949-2957.
- Hoffmann, M. A. M., and P. J. J. M. van Mil. 1997. Heat-induced aggregation of  $\beta$ -lactoglobulin: role of the free thiol group and disulfide bonds. *J. Agric. Food Chem.* 45:2942-2948.
- Manderson, G. A., M. J. Hardmann, and L. K. Creamer. 1999. Effect of heat treatment on the conformation and aggregation of  $\beta$ -lactoglobulin A, B and C. *J. Agric. Food Chem.* 46:5052-5061.
- Roefs, S. P. F. M., and K. G. de Kruif. 1994. A model for the denaturation and aggregation of  $\beta$ -lactoglobulin. *Eur. J. Biochem.* 226:883-889.
- Sawyer, W. H. 1967. Heat denaturation of bovine  $\beta$ -lactoglobulin and relevance of disulphide aggregation. *J. Dairy Sci.* 51:323-329.
- Shimada, K., and J. C. Cheftel. 1989. Sulfhydryl group/disulphide bond interchange reactions during heat induced gelation of whey protein isolate. *J. Agric. Food Chem.* 37:161-168.
- Xiong, Y. L., K. A. Dawson, and L. Wan. 1993. Thermal aggregation of  $\beta$ -lactoglobulin: effect of pH, ionic environment, and thiol reagent. *J. Dairy Sci.* 76:70-77.